Synthesis and characterization of fluorescent hollow silica nanoparticles: Control of size and metal incorporation for several nanotechnology applications

FINAL MASTER PROJECT DIRECTED BY

Jesús Santamaría Ramiro

Mª Pilar Lobera González

Nuria Moreno Berdejo

Master Degree in Nanostructured Materials for Nanotechnology Applications
September, 2015

Dpto. Ingeniería Química y Tecnología del Medio Ambiente
Instituto de Nanociencia de Aragón
Facultad de Ciencias
UNIVERSIDAD DE ZARAGOZA

ACKNOWLEDGMENTS

This report means the end of a year of work and the end of my master, however this would not been possible without the help of many people, so I would like to begin by thanking.

In the first place, thanks to Pilar Cea for her efforts in the difficult task to organizing and coordinating the master and thanks to Ciber-BBN for the award of the grant to carry out my final master project.

Thanks to my directors, Jesús Santamaría and Pilar Lobera for their guiding me in daily work, understanding and good advice. Also, thanks to Francisco Balas who gave me the opportunity to work with him and deposited on me the confidence to develop this project. And I can not forget to thank to the person who has been really my teacher in the laboratory, for his useful advice, his encouragement words and his enormous patience: Thanks Alberto Clemente.

Thanks to all members of NFP group: from all doctors who have taught and during this year to all my lab partners who make a great time, who are the responsibles of a nice environment in the laboratory and who have been my (necessary) coffee-time partners. Specially, thanks to Nuria Navascués for all her help and patience (and for all hours of TEM).

And finally,but no least, I want to thank to all my family, specially to my parents for their effort, their trust in me and their unconditional support and thanks to David to share and support me in the worst moments and to be the responsible for the best ones.

CONTENTS

1. INTRODUCTION

Nanotechnology is a emerging science focused in the design, fabrication and application of nanostructures or nanomaterials, and the fundamental understanding of the relationships between physical properties or phenomena and material dimensions.[1]

Materials at nanometer scale may exhibit physical properties distinctively different from that of bulk which have being exploited in different fields such as enviromental technology, improve electronic devices, catalysis, energy production or in biomedicine for early detection of diseases (bioimaging and biosensors) and treatment thereof (controlled drug delivery).[2]

Of all the existing nanomaterials, one of the most studied has been structures based on silicon dioxide (SiO_2) or commonly named silica. This compound consists in a polymer formed by tetrahedral SiO_4 units interconnected. Thanks to its versatility, non-toxicity, biocompatibility and wide range of applications, researchs based on this materials has growth in the last years (Fig. 1).

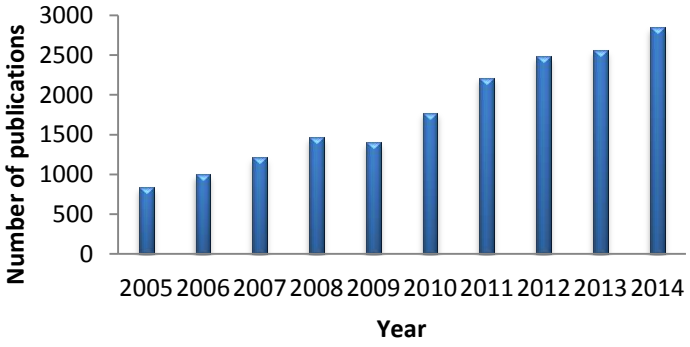

Fig. 1. Number of publications related to silica nanomaterials.[3]

Synthesis of silica nanostructures has been developed mainly by *sol-gel* process obtaining amorphous solids with high conectivity between SiO_4 units and higly hydroxylated surfaces. This method is based on a chemical process consisting in hydrolysis and condensation reactions between the initial precursors (alkoxy silicates) in different parts of the reaction mixture. In this manner the precursors begin to bind forming a colloidal structures (*sol*) and when this process continues, *sol* increases its viscosity and the polymeric chains grow up to macroscopic groups (*gel*)[4,5] (Fig. 2a). This method allows the modulation of the polimerization process according to pH and salt concentration in order to obatin different structures (Fig. 2b).

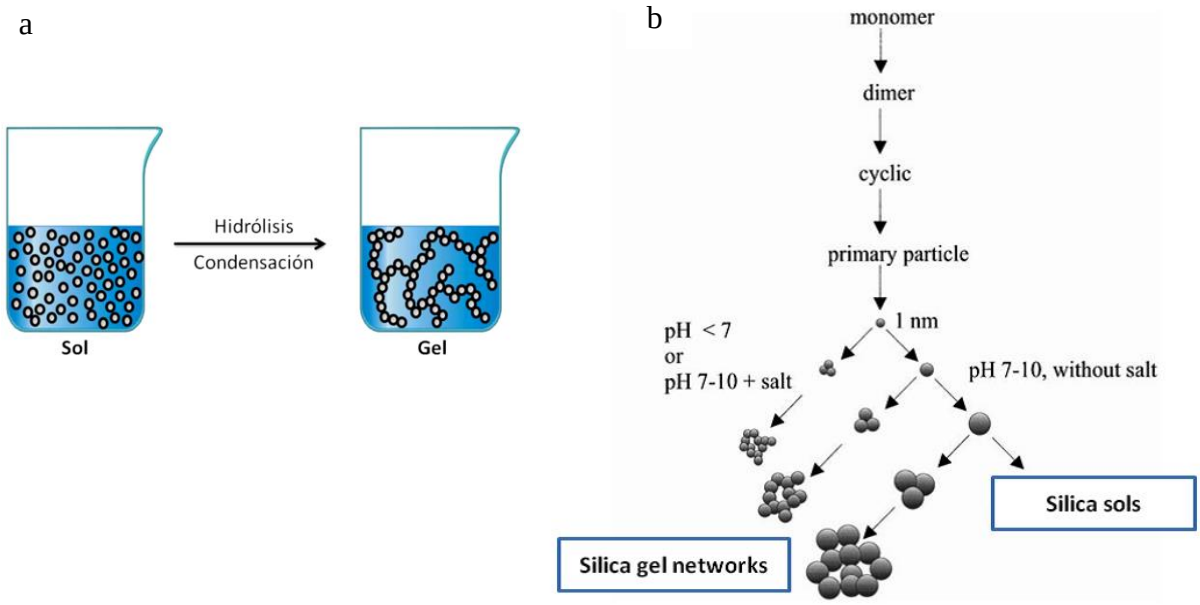

Fig. 2. a) Scheme of a *sol-gel* process.[4] b) Polymerization behaviour of silica describin the *sol-gel* process.[6]

According to their textural properties and morphology different types of silica-based nanostructures can be distinguished which could be used in several applications. The following scheme (Fig. 3) summarizes this classification.

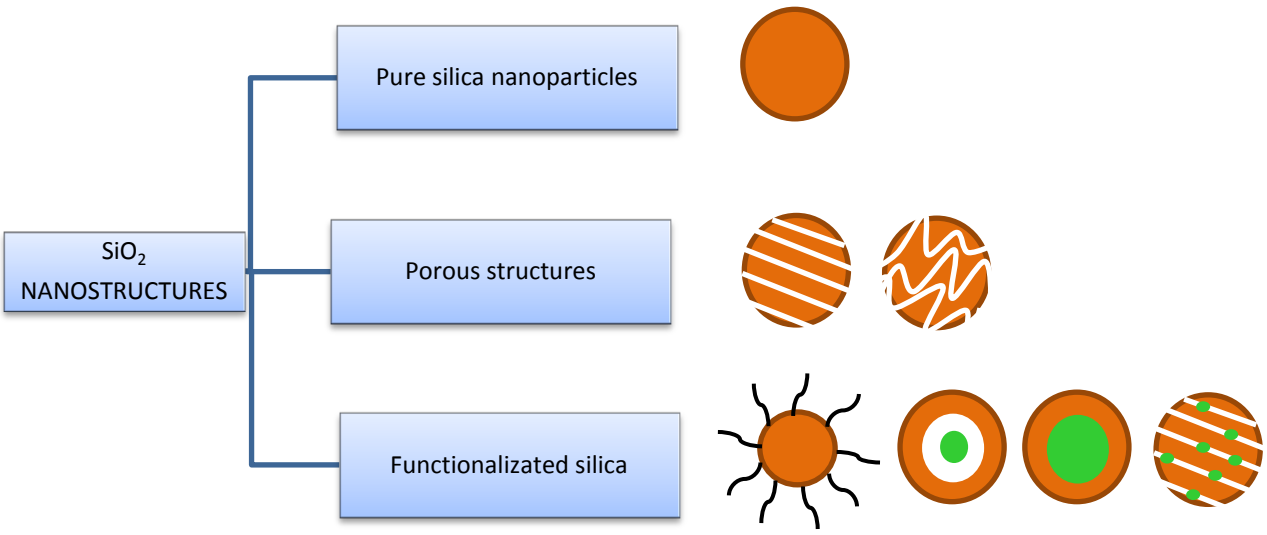

Fig. 3. Classification of different silica nanostructures.

- Pure silica nanoparticles

This type is referring to pure and dense spherical silica nanoparticles. Some of the widely used methods to synthesize pure silica nanoparticles are *sol-gel* process, reverse microemulsion and flame synthesis.

The *sol-gel* process is widely used to produce pure silica particles through systematic monitoring of reaction parameter. In this way, Stöber[7] synthesis is the most common method for synthesizing colloidal silica-based nanoparticles that are <100 nm in size. This method shows some disadvantages such as the nanoparticles are not uniform size and, due to the pH and the high concentrations of alcohols, this process is incompatible with doping some biomolecules such as proteins.

In reverse microemulsion, the surfactants molecules dissolved in organic solvents, forms spherical micelles. In presence of water, the polar head groups organize themselves to form microcavities containing water, which is often called as reverse micelles where a water-in-oil (w/o) microemulsion creates a nanodroplets system which acts a nanoreactors where a controlled synthesis is carried out. In comparasion to Stöber method, this synthesis needs a much longer time but shows highly efficient to the fabrication of spherical and monodispersed nanoparticles.[8] The major drawbacks of the reverse microemulsion approachs are high const and difficulties in removal of surfactants in the final products. However, this method was successfully applied for the coating of nanoparticles with different functional groups for various applications.[9]

Silica nanoparticles can also be produced through high temperature flame descomposition of metal-organic precursors. This process is also referred to as chemical vapor condensation (CVC). In a typical CVC process, silica nanoparticles are produced by reacting silicon tetrachloride, $SiCl_4$ with hydrogen and oxygen. Difficulty in controlling the particle size, morphology and phase composition is the main disadvantage of the flame synthesis. Nevertheless, this is the prominent method that has been used to commercially produce silica nanoparticles in powder form.[10,11]

- Porous structures

A porous material can be classfied according to the porous size in microporous (less than 2 nm), mesoporous (2-50 nm) or macroporous (greater than 50 nm). In the case of silica, mesoporous nanoparticles has been the most studied due to their properties such as mechanical resistance, chemical and thermal stability, biocompatibility, high surface area, high porosity with high pore volume and

modificable pore size.[12,13] All these characteristics allow the use of mesoporous silica in biomedical applications as drug delivery because the porous allow the storage of several molecules.

Some examples of mesoporous silica structures are MCM-41, SBA-15,SBA-16 or FDU-12.[4]

- Functionalized silica

There are different ways to functionalize so dense as hollow silica nanoparticles: by covalent linked on the surface or within the structure of the nanoparticle.

The high concentration of –OH groups on the surface of silica nanoparticles allows the possibility of its surface modification by covalent bond with several molecules forming hybrid structures with different functionalities.[4]

On the other hand, silica precursors can be convalently modified with different molecules, such as luminophores, in order to synthesize functionalizated nanoparticles which can be used as luminiscent markers.[14] Some of these luminophores are fluorescein isothiocyanate (FITC), rhodamine, cyanine or ruthenium complexes. This project has been focused in the use of FITC (Fig. 4) as luminophore. It is a organic molecule with fluorescence properties belonging to the group of xanthenes and shows very high molar absorptivity at 488 nm and high quantum yield with a emission spectra at 490 nm.[15]

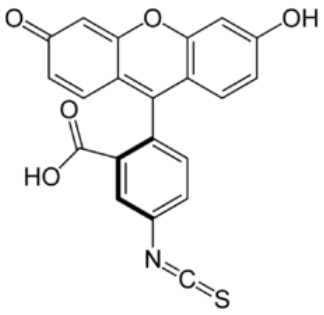

Fig. 4. Structure of FITC.

Finally, in the case of porous and hollow silica nanoparticles, the synthesis of nanohybrids is a way to obtain functionalized silica nanostructures. For this end, several useful loads such as metal nanoparticles, quantum dots or drugs can be introduced inside of cavities of silica nanoparticles. These useful loads could have magnetic or optical properties, could be used in catalysis, as bactericide, etc.

Traditionally, two approaches can be followed to synthesize nanohybrids: first using a template which is covered by porous silica and after the template is removed generating a hole where useful loads can be introduced (Fig. 5a) or second, starting from the useful load, cover it by a template and after synthesize a shell of silica around the template. Finally, the template is removed remaining the useful load inside the structure (Fig. 5b). In this way these generated nanohybrids can act as transport vehicles.[16]

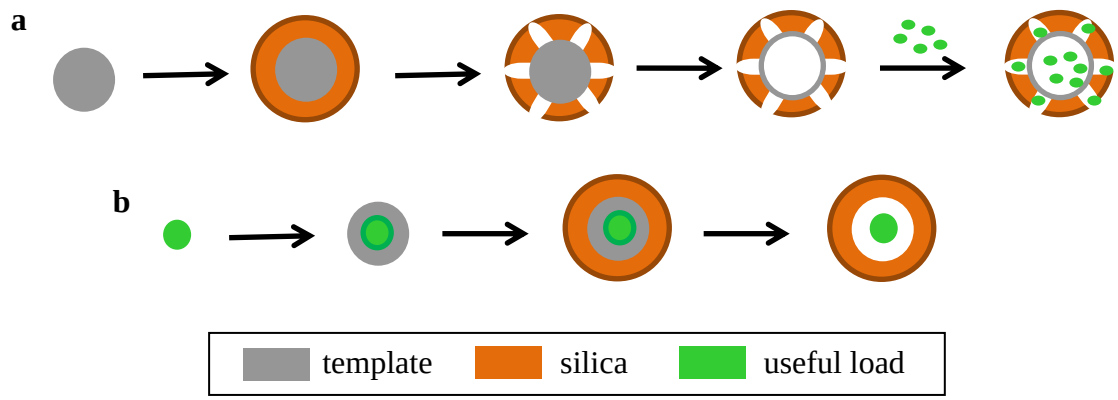

Fig. 5. Scheme of the most common processes to introduce useful loads in hollow silica nanoparticles.

Even so, the controllable synthesis of nanohybrids with a narrow particles size distribution by a simple and scalable method is still a great challenge.[17]

In this project, we present one-step synthesis of monodisperse silica-based nanohybrids. The proposed method started from fluorescence dense silica nanoparticles obtained by microemulsion, followed by the introduction of different useful loads in one step, taking advantage of the hollowing process.

2. OBJECTIVES

The core idea of this master final project was to study and control the process of formation fluorescent hollow silica nanoparticles proposing a mechanism to explain this phenomena. To that end, different experiments was carried out in order to find out the influence in the hollowing process of both synthesis routhe of fluorescent SiO_2 nanoparticles and effect of aging conditions.

In addition to primary objective in this final master project, and taking advantage of the control of the hollowing process, series of experiments were conducted in order to introduce several useful loads obtaining fluorescent and functionalized silica-based nanohybrids which can be used in different applications. Finally, an overview of potential applications for synthesized silica-based nanohybrids in different fields as selective catalyst, markers, bactericide, photonics, etc. were addressed.

3. METHODOLOGY

3.1 CHEMICALS

Tetraethyl orthosilicate (TEOS, 98%, Aldrich, St. Louis MO), 3-aminopropyl ethoxysilane (APTES, 99%, Aldrich), ethanol (EtOH, 99%, Aldrich), cyclohexane (99%, Aldrich), n-hexanol (99%, Aldrich), polyoxyethyleneoctyl phenyl ether (TX-100, 99%, Aldrich), 3-(trihydroxysilyl)propylmethylphosphonate (THPMP, 42%, Aldrich) and Benzilic alcohol (BzOH, Aldrich) were used as received. Milli®Qwater (Millipore, Billerica MA) and ammonium hydroxide (NH_4OH, 25-28% solution in water, Aldrich) were used as reagents for the hydrolysis of silicate precursors. Fluorescent label fluorescein 6-isothiocyanate (FITC, 99%, Aldrich) was used without previous purification. Chloroauric acid ($HAuCl_4$, Aldrich), chloroplatinic acid (H_2PtCl_6, Aldrich), silver nitrate ($AgNO_3$, Aldrich) and iron (III) acetylacetonate ($Fe(acac)_3$, Aldrich) were used as metal sources, and sodium borohydride ($NaBH_4$, Aldrich) as reductant agent.

3.2 SYNTHESIS FLUORESCENT SiO_2 NANOPARTICLES

Monodisperse fluorescent silica nanoparticles was synthesized by a modification of the single emulsion method.[18] The first step was the synthesis of fluorescent silane precursor (FITC-APTES conjugate) (Fig. 6). To that end, 5.7 mg of FITC were disolved in 1 mL absolute ethanol and 73 µL APTES were added under Ar atmosphere. The mixture was stirred in dark during 12 h to obtain FITC-APTES precursor where FITC is covalently attached to APTES by a stable thiourea linkage.

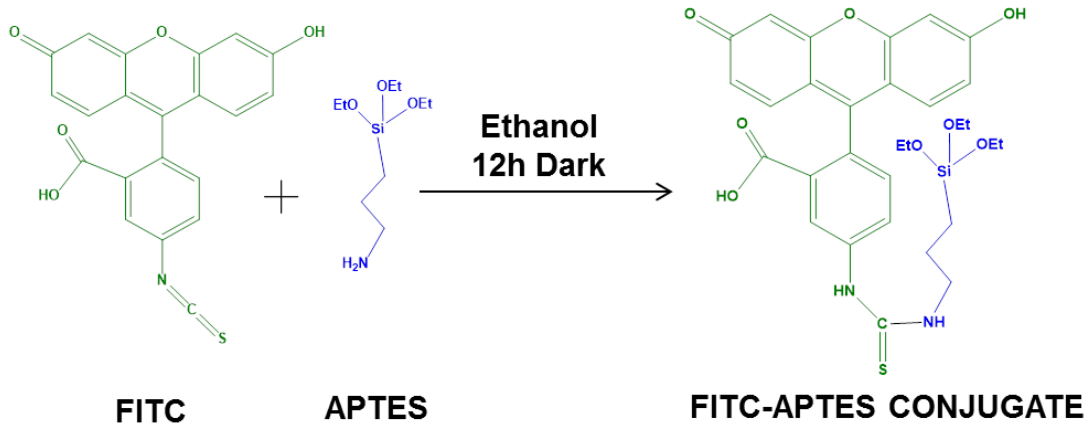

Fig. 6. Formation of FITC-APTES conjugate.

The second step was the preparation of a water-in-oil (w/o) microemulsion formed by 7.7 mL cyclohexane, 1.7 mL Triton X-100, 1.6 mL 1-hexanol and 0.34 mL water and stirred during 30 min. After, sequentially each 10 minutes 100 µL of FITC-APTES conjugate, 100 µL TEOS, and 100 µL NH_4OH were added. After 30 min, 15µL of THPMP were added and the mixture was kept under magnetic stirred in the dark at 25ºC for 24h, leading in a highly water-dispersible fluorescent SiO_2 nanoparticles. The synthesis (Fig. 7) was carried out by the hydrolysis and co-condensation reaction of TEOS and FITC-APTES conjugated in presence of ammonium hydroxide which provides a basic medium and acted as catalyst.[19]

Finally, as-synthesized nanoparticles were submitted to several cycles of centrifugation (10000 rpm, 10 min), washed with a mixture of alcohols (methanol, 2-propanol, ethanol and water) to remove the surfactant and dispersed with sonication device (80 W, 2 min).

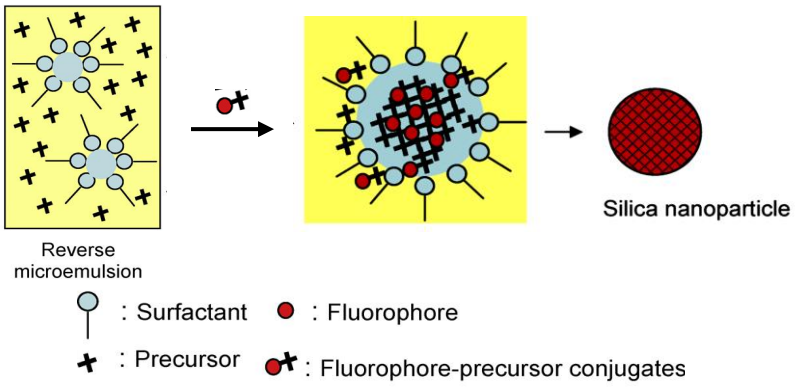

Fig. 7. Scheme of the synthesis process.[15]

3.3 SYNTHESIS HOLLOW FLUORESCENT SiO_2 NANOPARTICLES

To create fluorescent hollow silica nanoparticles, they were isolated by centrifugation and re-suspended in milli®Q water to reach a concentration of 1 mg/mL. This aqueous suspension was aged by their stored in the dark at 25ºC during a certain period of time.

In order to understand and control the hollowing process, the evolution of the hole was monitored along the time, and also different modifications in the synhtesis routhe and aging conditions were tested.

Different modifications in the synthesis routhe of silica nanoparticles were carried out in order to study their influence in the hollowing process, following by the same aging process of the resulting aqueous suspension (storaged in dark at 25ºC during 5 days). As a first approach the water/Si ratio used in the synthesis was changed. The original synthesis was carried out with a ratio water/Si of 30 and the following with 40 and 50. The second approach was based on replacing the microemulsion media (Cyclohexane, TritonX-100 and 1-hexanol) by the same volume of ethanol to perform the synthesis of fluorescent SiO_2 nanoparticles through a *sol-gel* method. The third approach consisted in synthesizing non-fluorescent silica nanoparticles. To that end, FITC-APTES conjugated was replaced by APTES in one case, and without anything silane precursor in the other, being TEOS the only Si source used in the synthesis.

As said above, the influence of aging conditions in hollowing process was exploired. The temperature effect was checked into two approaches: subjecting a suspension of fluorescent silica nanoparticles in ethanol/water media (1:1) at reflux at 80ºC during 5 hours on one hand; and aging an aqueous suspension of fluorescent silica nanoparticles at 4ºC during 5 days. The pH effect was studied by using an aqueous suspension of silica nanoparticles at different pHs (2, 3, 6 and 9) achieved by addition of HNO_3 or NaOH during the aging process. Finally, the aging process was carried out using as aqueous media a solution of NaCl in order to find out whether the presence of ions could affect hollowing process.

3.4 METAL INCORPORATION

In order to obtain silica-based nanohybrids, fluorescent hollow silica nanoparticles were formed in a aqueous media containing the metal precursor. Different metal sources, such $HAuCl_4$ (1 mM), H_2PtCl_6 (1 mM), $AgNO_3$ (1 mM) or $Fe(acac)_3$ (1.89 mM) were used. The fluorescent SiO_2 nanopartcles were storage in this solution for 5 days at 25ºC in dark.

After that, in the samples containing Au, Ag and Pt, 4-times molar excess $NaBH_4$ was used to reduce metallic cations to form metal nanoparticles in the core of the silica nanoparticles. Finally, the metal-silica hybrids were isolated for small free metal nanoparticles by few cycles of fractional centrifugation (10000 and 1000 rpm, 15 min).

While the sample containing the Fe precursor, the suspension obtained after the aging process was centrifugated and washed with milliQ®water to remove iron ion excess. Then, the isolated nanoparticles were dried by liophilization during 24 hours. After that, 20 mL benzyl alcohol was added in a reduced pressure set up (Fig. 8) and was stirred during 30 min. Finally, the nanoparticles alcohol based suspension was exposed to atmospheric pressure. Then it was submited at microwave treatment[20] (1st step: 3 min-1000W ramp to 200ºC, 2nd step: 7 min-1000W at 200ºC) in a Milestone Ethos Plus equipment to obtain magnetic silica nanoparticles. Finally they were purified by several cycles of centrifugation (10000 rpm, 10 min) with ethanol.

Fig. 8. System at reduce pressure during the addition of benzyl alcohol.

3.5 CHARACTERIZATION TECHNIQUES

TRANSMISSION ELECTRON MICROSCOPY

Transmission Electron Microscopy (TEM) is a technique where a beam of electrons bombs a sample (a drop of a suspension of nanoparticles put on a cooper grid) interacting with it. A part of these electrons pass though the sample generating an image of the sample.

This technique has been used to characterize the morphology and size of the nanoparticles studied in this project. The equipment used was a Tecnai T20 (FEI Co,

Hillsboro OR) electron microscope at a 200 kV in TEM mode and Tecnai F30 with STEM mode and analysis by enegy dispersive X-ray spectroscopy (EDX).

UV-VIS ABSORBANCE

UV-Vis absorbance spectrophotometry is a technique based on measure the absorption of electromagnetic radiation by some molecules called fluorophores. In this project, absorbance measurements was carried out in order to characterize the composition of the nanoparticles and the supernatants obtained during the hollowing process. This technique helps us to elucidate a mechanism of hollow formation thanks to the optical properties of the different chemical precursors of fluorescent silica nanoparticles. Also, we can obtain information about the different metals which were introduced inside the particles, due to some of them shows absorption band in the UV-Vis range.

The equipment used to made these measures was Varian Cary 50 Spectrophotometer.

PHOTOLUMINESCENCE

Photoluminescence is a property of the silica nanoparticles synthesized and metal-silica nanohybrids due to the incorporation of the fluorophore FITC and consists in the emission of electromagnetic radiation at certain wavelengths. Fluoresecence measurements give information about the stability along the time of this nanoparticles and helps to determine the mechanism to hollow formation.

The measurements were carried out in Perkin Elmer LS 55 Fluorescence Spectrometer.

NITROGEN ADSORPTION ISOTHERM: BET

Nitrogen adsorption is a technique based on the capacity of adsorption and desorption of nitrogen gas by micro and mesoporous materials. In this way, information about the size and shape of the porous of the material can be obtained.

In this project, BET technique has been used to measure textural properties of silica nanoparticles before and after of their aging in water. The equipment used was Tristar 3000 V 6.08, Micromeritics Corp., Noncross, GA.

^{1}H-NUCLEAR MAGNETIC RESONANCE

Nuclear magnetic resonance (NMR) is a physic phenomena based on the interaction between the nucleus of an atom and a electromagnetic field. In our case, the chemical element studied was hydrogen in order to clarify the morphology evolution process of silica nanoparticles.

NMR measurements were performed using a 2 AVANCE-400 and Bruker Avance 500 equipment.

X-RAY PHOTOELECTRON SPECTROSCOPY (XPS)

X-Ray photoelectron spectroscopy (XPS) is a technique used to determine the chemical composition of a sample. This technique was used to determine the atomic metal/Si concentration ratio of the fluorescent hollow silica-based nanohybrids.

The equipment used was a Krapts AXIS Ultra DLD system with a monochromatized Al Ka beam at 1466 eV.

4. RESULTS AND DISCUSSION

4.1 STUDY OF THE HOLLOWING PROCESS

When a sample of fluorescent silica nanoparticles (Fig. 9a) was aged in water during 5 days, fluorescent hollow nanoparticles were obtained (Fig. 9b).

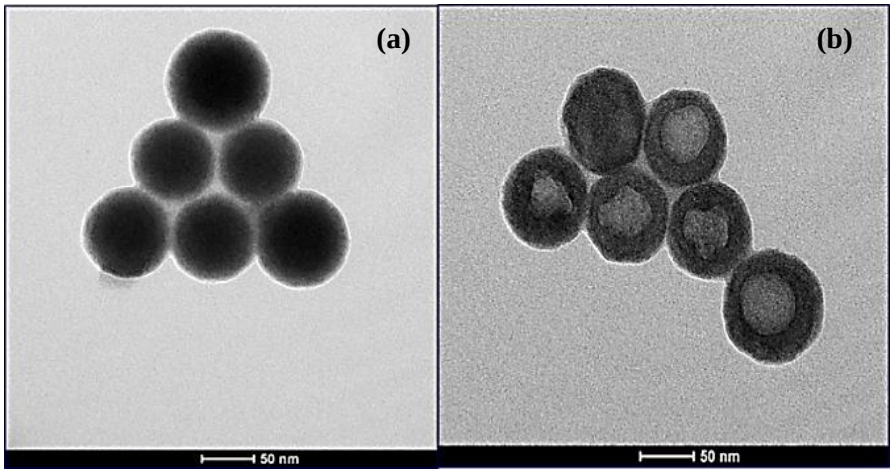

Fig. 9. TEM images of fluorescent silica nanoparticles after their storage during 5 days a) in ethanol b) in water.

EVOLUTION OF HOLE FORMATION

This process was followed along the time in order to study the evolution of the hole formation.

During the hole formation process, the evolution of interior void diameter (Dh) was monitored during a month by TEM analysis (Fig. 10). Representative TEM image (Fig. 10a) indicates formation of solid silica nanoparticles with uniform particle size of 60 ± 8 nm (Dp). Fig. 11b and Fig. 11c show how the size of the hole was increased progressively along the time up to 40 nm, mantaining the size of the nanoparticle, until the formation of a stable suspension of hollow fluorescent nanoparticles even a month after storage in aqueous media.

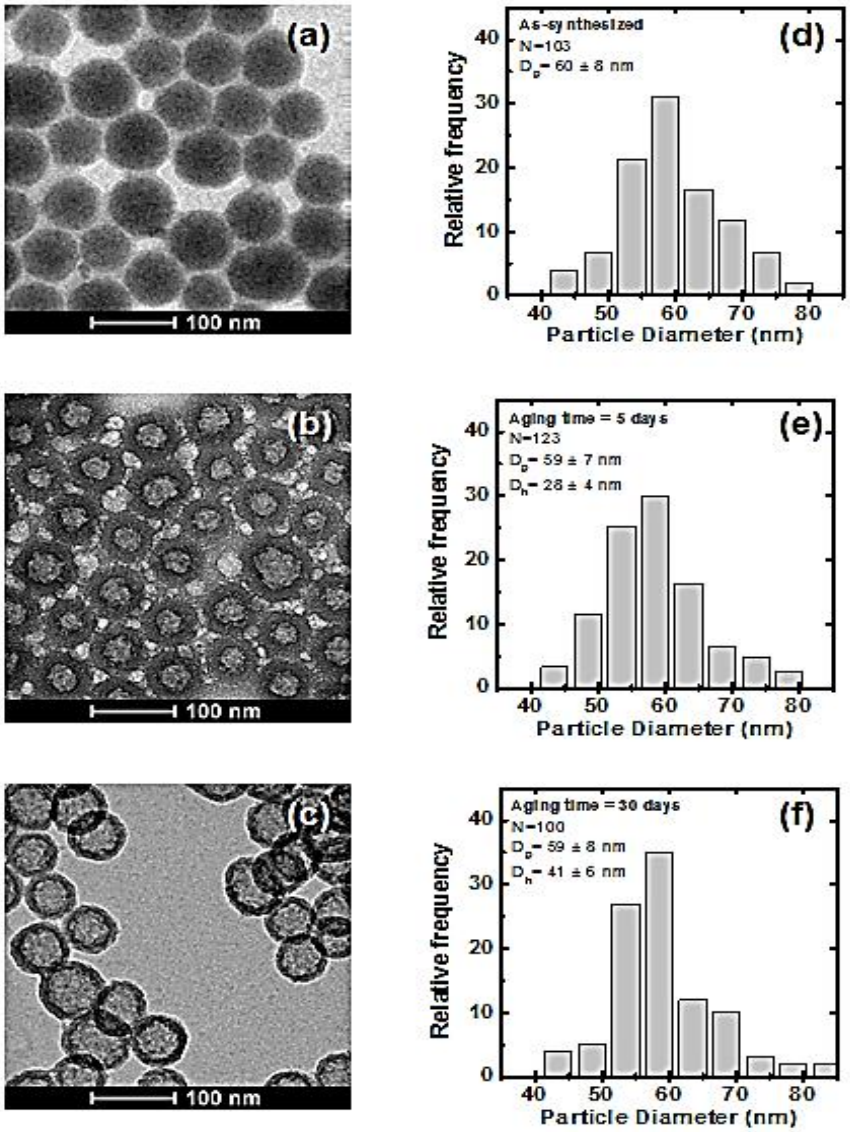

Fig. 10. (a,d) TEM image of fluorescent dense silica nanospheres with the histogram showing particle size distributions were shown. (b,c,d,f) TEM image of fluorescent hollow silica nanosheperes at different aging time and histograms showing particles size distribution were shown.

TEMPERATURE EFFECT

The fluorescent SiO_2 nanoparticles were suspended in an ethanol-water mixture (1:1) and refluxing for 5 hours (T~80ºC). Fig. 11a shows similar hole evolution than the obtained after storage in aqueous media during 5 days at 25ºC in dark. Moreover, the fluorescent properties remained unchanged. So, the hollowing process can be accelerated with the increase of temperature due to higher diffusivity of water molecules into the pristine SiO_2 nanoparticles. However, the storage in aqueous media at lower temperatures do not slow down the hollowing process. Fig. 11b shows that mean void

diameter obtained after an aging process in aqueous media during 5 days at 4ºC in dark was similar than the obtained after the same aging process at 25ºC.

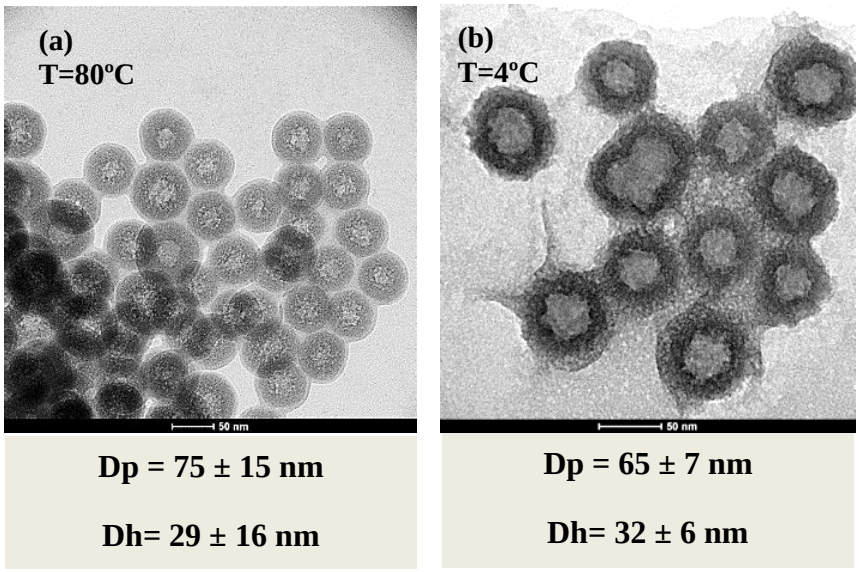

Fig. 11. Hollow fluorescent silica nanoparticles formed by aging in a) 80ºC at reflux during 5 hours b) at 4ºC during 5 days.

pH EFFECT

Fluorescent SiO_2 nanoparticles were aging during a month at 25ºC in dark using aqueous solutions with different pH conditions. Fluorescent silica nanoparticles were showed at TEM (Fig. 12). The particle size distribution remained unchanged around 56 nm with the pH used in the aging medium. Futhermore a retardation of complete hydrolysis of siloxanes groups located in the core of the silica nanoparticles was observed at pH=2, and no formation of the inner hole is observed after a month of aging (Fig. 12a). However in the same time of aging, an increase in the pH of the aging medium accelerates the hydrolysis rate of inner siloxanes groups and enables the formation of an inner hole up to 41 nm. As expected, the SiO_2 nanoparticles aged at pH=9 were degradated. Thus, the fluorescent silica nanoparticles can be tailor-made depending the pH conditions of aqueous media used for their aging.

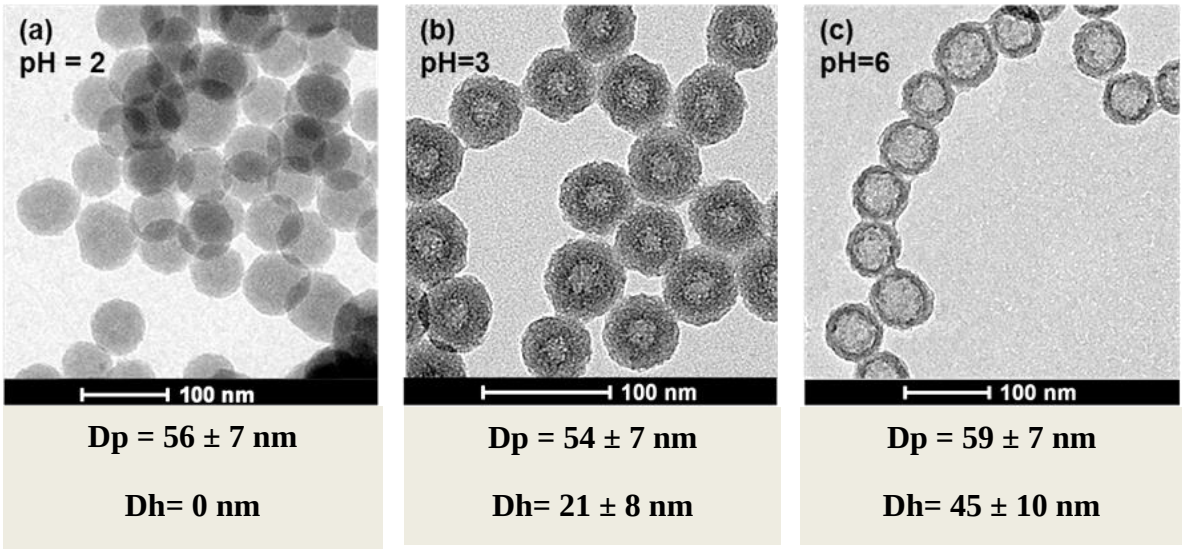

Fig. 12. Evolution of hollowing process at different pHs.

IONIC STRENGTH EFFECT

5-days aging test were realized increasing the concentration of ions in the aqueous media used, specifically a ionic strength of I = 0.0342 M was used. The results shown that when the concentration of ions was increased the formation of the hole was delayed, even inhibited (Fig. 13a). Moreover, only an early stage of the hollowing process was observed when the aging process of the SiO_2 nanoparticles was accelerated by refluxing them for 5 hours in a ethanol-water mixture (1:1) with the same ionic strength of than in the previous experiment (Fig. 13b). Higher concentration of ions in the aging aqueous media were related with a delay in the formation of hollow silica nanoparticles.

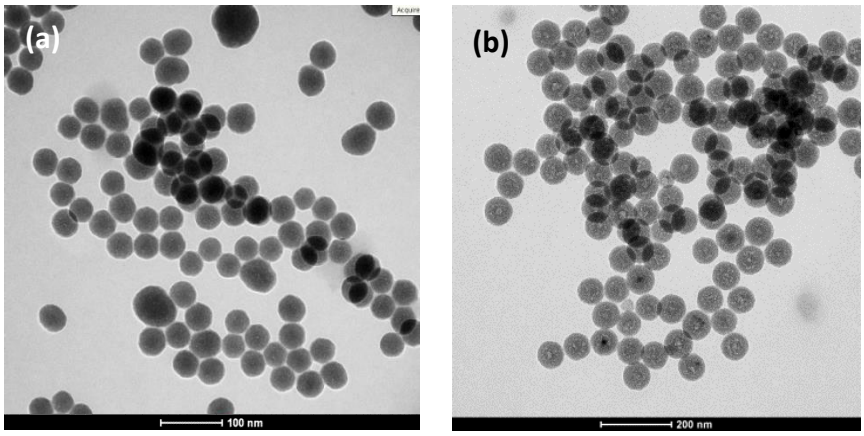

Fig. 13. Fluorescent silica nanoparticles (62 ± 6 nm) after aging in NaCl solution (I=0.0342 M) during a) 5 days b) 5 hours at reflux.

INFLUENCE OF SYNTHESIS ROUTHE OF FLUORESCENCE SILICA NANOPARTICLES

Diverse modifications in the synthesis routhe of fluorescent silica nanoparticles were carried out in order to study their influence in the hollowing process. In all cases, the SiO_2 nanoparticles were aging in aqueous media during 5 days at 25ºC in dark.

First, the water/Si ratio (R) used in the synthesis of the fluorescent SiO_2 nanoparticles was increased. The results showed that an increase of the water/Si ratio used in the synthesis (eg. an increase in the amount of water) retards the hole formation being the diameter lower (Fig. 14).

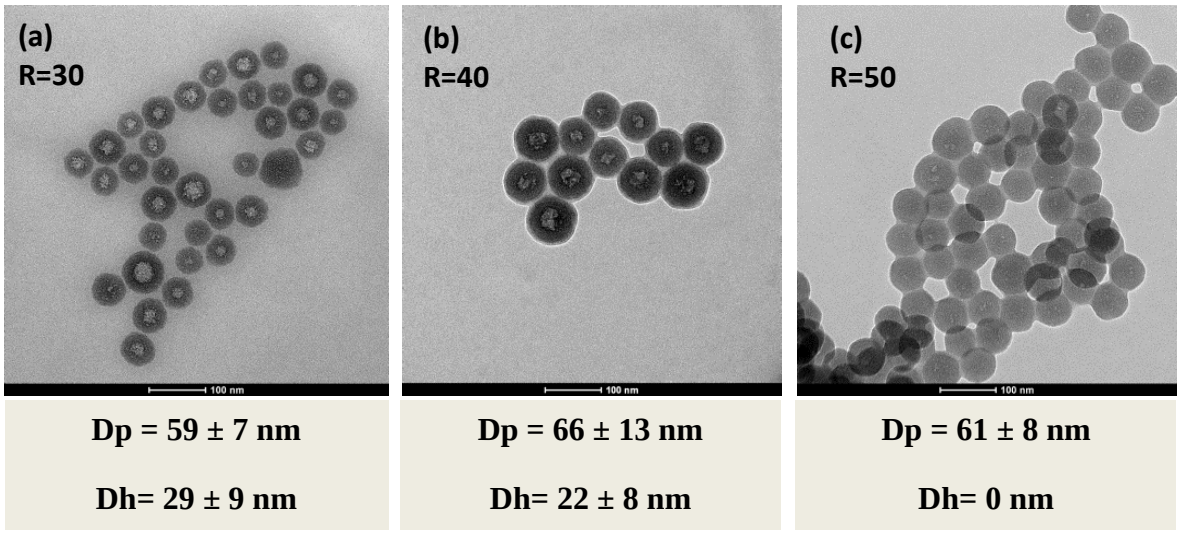

Fig. 14. Evolution of fluorescent silica nanoparticles at different water/Si synthesis ratios a) 30, b) 40 and c) 50 after 5 days of aging time.

As second approach, the microemulsion media (Cyclohexane, TritonX-100 and 1-hexanol) was replaced by the same volume of ethanol to perform the synthesis of fluorescent SiO_2 nanoparticles through a *sol-gel* method. According to Fig. 15, the microemulsion is responsible for obtaining a monodisperse fluorescent SiO_2 nanoparticles, controlling their size and shape, while the synthesis carried out through a *sol-gel* method in ethanol solution turned out to have SiO_2 nanoparticles with great polydispersity. Two populations were identified: one of 156 ± 28 nm and another of 69 ± 13 of size. Also, the hollowing process was studied in these polydispersed nanoparticles obtained by *sol-gel* method. After 5 days of aging in water only bigger nanoparticles showed inner hole (Fig. 15).

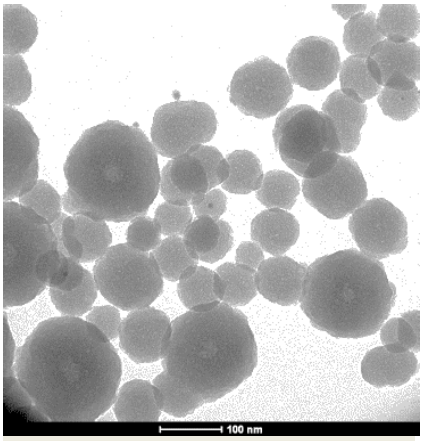

Dp_{higher} = 156 ± 28 nm

$Dp_{smaller}$ = 69 ± 13 nm

Dh = 26 ± 10 nm

Fig. 15. Two populations of fluorescent silica nanoparticles synthesized in ethanol media after 5 days of aging in water. Holes are only observe in higher nanoparticles.

Finally, non-fluorescent SiO_2 nanoparticles were synthesized and their hollowing process was studied. Two approaches were carried out: first, using only APTES solution as conjugated and second, without any conjugated molecule.

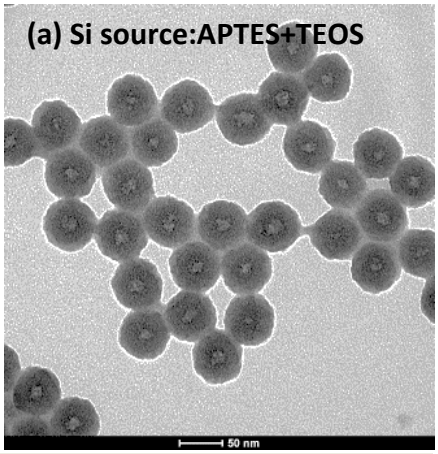

Dp = 55 ± 3 nm

Dh= 11 ± 2 nm

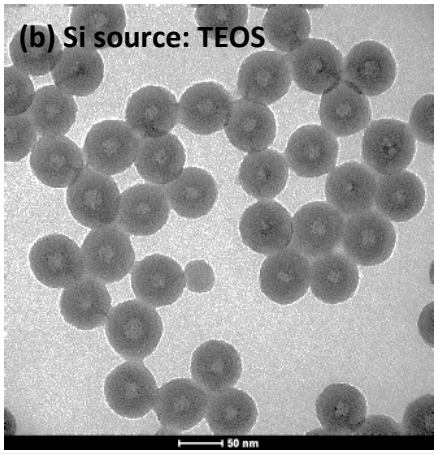

Dp = 52 ± 6 nm

Dh= 14 ± 2 nm

Fig. 16. Non-fluorescent silica nanoparticles using as Si source a) TEOS and APTES b) only TEOS.

In both cases there are not difference in the size and shape regarding those obtained in the original synthesis of fluorescent SiO_2 nanoparticles. Fig. 16 shows the hollow SiO_2 nanoparticles after 5 days of aging time in aqueous media. In both cases, the diameter of the hole is slightly less than in the orginal particles (from 11 to 14 nm).

This phenomena could be due to the non presence of large hydrophobic groups allowing higher number and better packing of the hydrolyzable chains (which contains Si-O-Et groups).

MECHANISM OF FORMATION OF FLUORESCENT HOLLOW SILICA NANOPARTICLES

The analysis of all of this experiments and the characterization techniques allowed to propose a mechanism to explain the formation process of hollow SiO_2 nanoparticles.

Role of organic and siloxane groups was crucial in the formation of hollow silica nanoparticles as well the amount of water used during the synthesis. The process started with the synthesis of fluorescence silica nanoparticles in a microemulsion (w/o) media. As shown above, this procedure allowed the obtention of nanostructures with controlled shape and size. A nanodroplets system was formed which acted a nanoreactors where a synthesis of the nanoparticles was carried out being regulated the accesibility of each reagent according to their hydrophobic or hydrophilic character (and their stearic impediment).

Once NH_4OH was added into the microemulsion, TEOS and FITC-APTES conjugate (as silica sources) were catalytically hydrolyzed to form silanol groups, moved into the water droplet in the microemulsion and co-condensed to form an organic-inorganic siloxane framework. These seminal siloxane groups were assumed to crosslink [SiO_4] tetrahedra with [O_3Si-R] units, where R is FITC molecules covalently linked to APTES by thiourea bonds (Fig. 17). Since these condensation reactions occurred in the aqueous droplets within the microemulsion, it could be proposed that more hydrophobic [O_3Si-R] units were mainly oriented inward as the silica nanoparticle was growing. This feature could in turn reduce the access of water molecules to the inner part of the forming nanoparticle. In such way, water becomes the limitant reagent and resulting in an inefficient hydrolysis and condensation reactions during formation of siloxane framework. That is, nanoparticles are formed by a dense shell of polymerized SiO_2, while inside the nanoparticle, where the most hydrophobic groups are oriented, there are etoxi groups which have not been hydrolyzed. So, the core of the nanoparticles is formed by a silice gel with lower density.

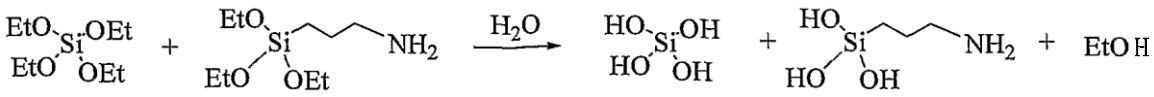

Fig. 17. Hydrolysis of silica precursors APTES and TEOS.

Density profiles obtained by STEM shows the existence of a lower density region in the inner zone of the fluorescent silica nanoparticles. The presence of this region was also confirmed by BET measures (Fig. 19) when the adsorption and desorption of nitrogen by dense and hollow nanoparticles could be compared. First, the obtention of porous silica nanoparticles with a porous size around 3-4 nm and the presence of a inner hole hollow were confirmed. The surface area of the hollow SiO_2 nanoparticles are 292 m^2/g, which are larger than those of dense one, 122.9 m^2/g. A steep decline in the adsorbed nitrogen at a relative pressure of 0.5 in the hysteris loop, allowed to propose a bottleneck structure connecting the porous and the inner hollow region.

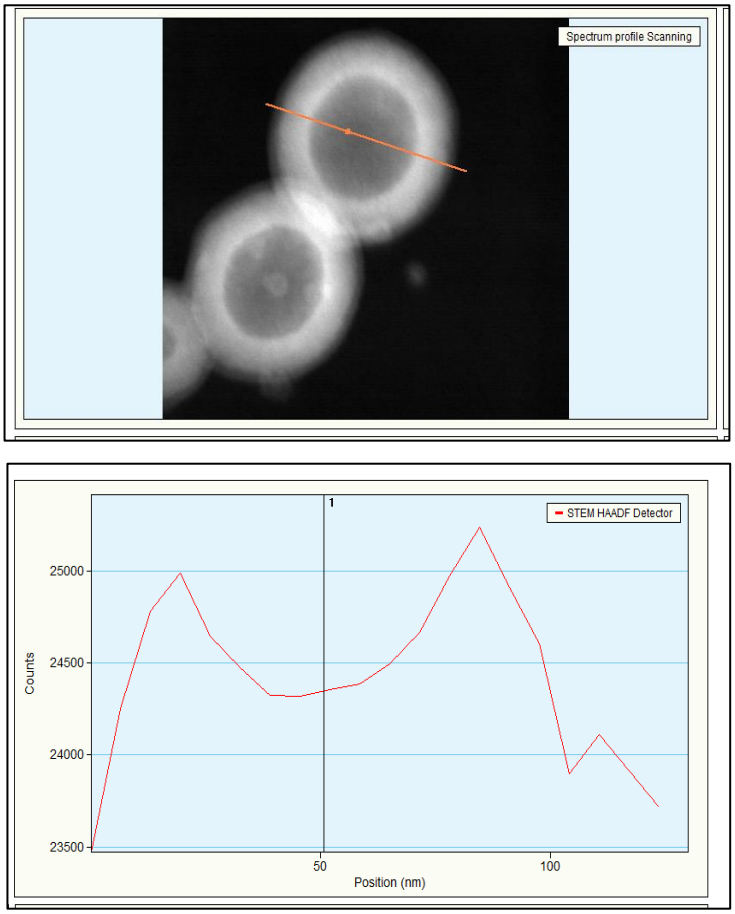

Fig. 18. Density profile of fluorescent silica nanoparticles after 5 days of aging in water.

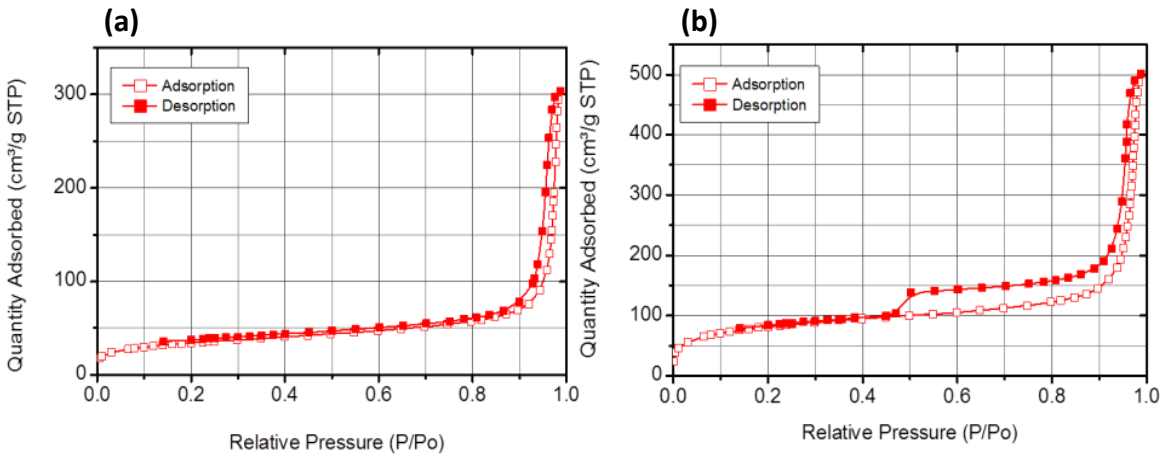

Fig. 19. Isotherms of nitrogen adsorption and desorption for a) dense and b) hollow fluorescent silica nanoparticles

When fluorescent silica nanoparticles were aged in aqueous media, water molecules diffuses through the inner part of the nanoparticles and the hydrolysis of organosiloxanes were complete and some R groups were formed. This R groups were released through the outer liquid media, so the interior void was created. In order to check what molecules left the nanoparticles during the hollowing process, as-synthesized fluorescent silica nanoparticles were aged in aqueous media and the supernatants obtained at different times were measured by UV-Vis spectroscopy.

The spectra of the supernatants demonstrated a broad absorption peaks at 490 nm (Fig. 20). In all cases, the intensity of absorption peak gradually increased with the aging.time. To clarify the nature of absorbing species, the UV-Vis spectrum of the dye molecule and FITC-APTES conjugate in aqueous medium at pH 6.5 were measured. The FITC spectrum has distinctive features of dianion fluoresceine in polar solvents such as water or ethanol. It has its main absorption peak at 490 nm and has a very weak absorption in the region of 350-400 nm. The FITC-APTES conjugate spectrum has a wide absorption with a maximum at 490 nm, a slight absorption in the region of 350-400 nm. It can be observed that the absorption peak of the supernatants was similar at the FITC-APTES peak, so probably, part of these molecules leave the nanoparticle during the hollowing process.

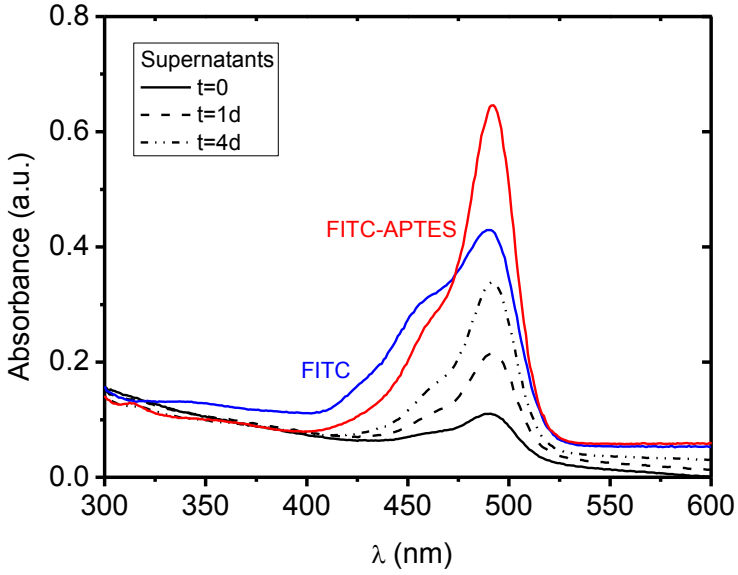

Fig. 20. UV-VIS spectra of FITC (blue), APTES-FITC-APTES conjugated (red) and supernatants at different aging times (dotted lines).

In addition, fluorescence measures were realized at different aging times (Fig.21). The results showed an increased emission at 516 nm where FITC-APTES conjugated shows maximum emission. This is due to fluorescent FITC-APTES molecules left the silica structure during the aging time and they were free in solution where their emission was higher than when they were inside the particle. This result is consistent with those obtained by UV-Vis.

Once the hollowing process was finished, the fluorescence emission of a water suspension of hollow nanoparticles was stable over time. This means that fluorescent hollow SiO_2 nanoparticles are stable strucutures where the hydrolysis reaction does not taking place because all the Si-O-Et groups had been hydrolyzed and where fluorescent molecules do not leave the nanoparticle structure.

Finally, the supernatants were analyzed by ^{1}H-NMR (*see annex 1*) and they were compared with the spectra obtained for APTES, FITC and FITC-APTES conjugated in deuterated methanol. In this case, the presence of a different peaks corresponding to ethanol molecules (1.17 and 3.65 ppm) confirmed that the hydrolysis reaction had been carried out during the aging time. However, due to poor detection limit of the equipment, the presence of peaks from aromatic rings corresponding to FITC-APTES conjugate (between 7 and 7.5 ppm) was very weak, so their concentration in solution

was very low. Although it can detected by UV-Vis and fluorescence measures due to the high molar absorptivity and high emission of this molecule.

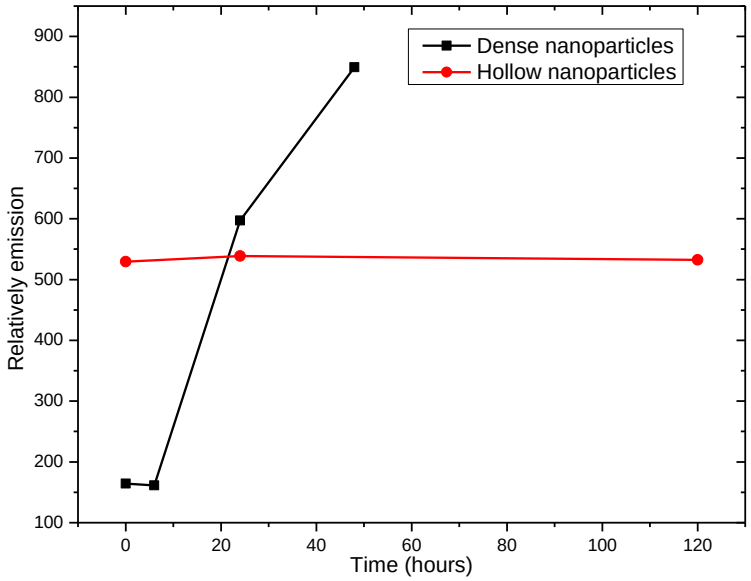

Fig. 21. Emission at 516 nm showed by dense (black) and hollow (red) nanoparticles in water.

4.2 METAL INCORPORATION

Once a through knowledge of the synthesis of mechanism of fluorescent hollow silica nanoparticles was obtained, the main challenge was the synthesis of silica-based nanohybrids which contained useful loads.

The different useful loads which could be introduced in the fluorescent hollow silica nanoparticles were metallic silver, gold and platinum nanoparticles in order to form nanohybrids. This strategy gave the chance to develop silica-based nanohybrids with a metal core following a novel synthesis route. Our approach allowed in situ growth of metal nanoparticles during the formation of the internal void of the silica nanoparticles. To that end, the synthesis of hollow silica nanoparticles was performed by aging the nanoparticles in an aqueous solution containing the metal precursor for 5 days. This enables the diffusion of metal cations through the micropores in the sphere to the inner part of the silica nanoparticles. After that an excess of $NaBH_4$ as reducing agent was added and the silica nanoparticles were kept for 2 h. And the metal nanoparticle formation took place by nucleation and growth of M(0) atoms. The simultaneous formation of silica shell avoided further growth of nanoparticles, acting as a template, and finally stabilized them.

The obtained nanohybrids were characterized by TEM (Fig. 22) and STEM (Fig. 23) where the presence of each metal was checked.

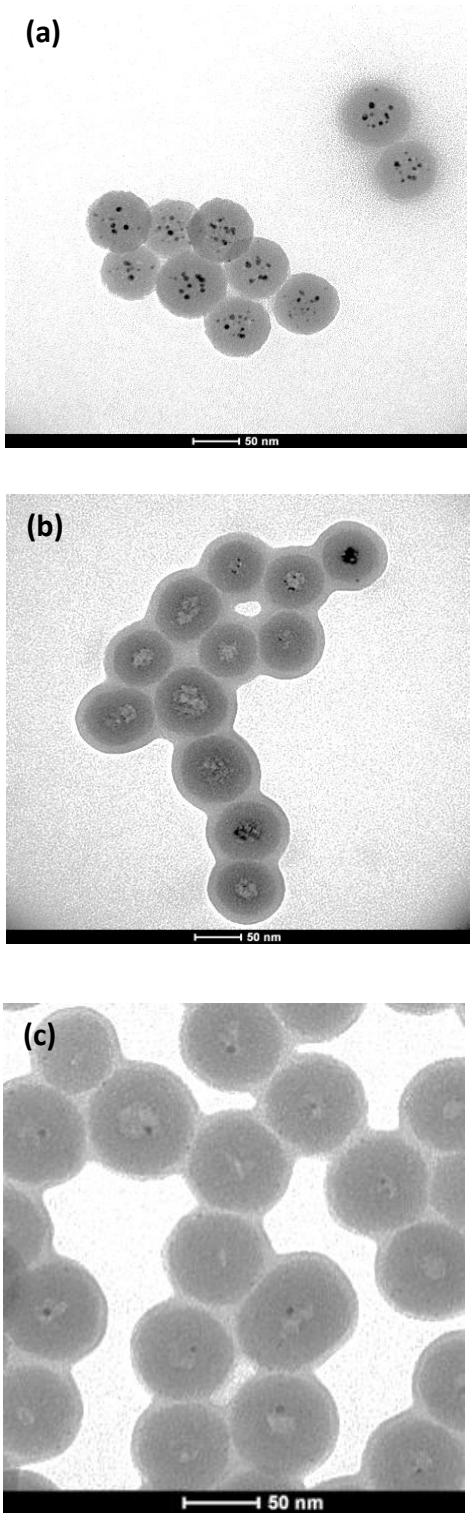

Fig, 22.TEM images of a) gold b) silver and c) platinum silica-based nanohybrids.

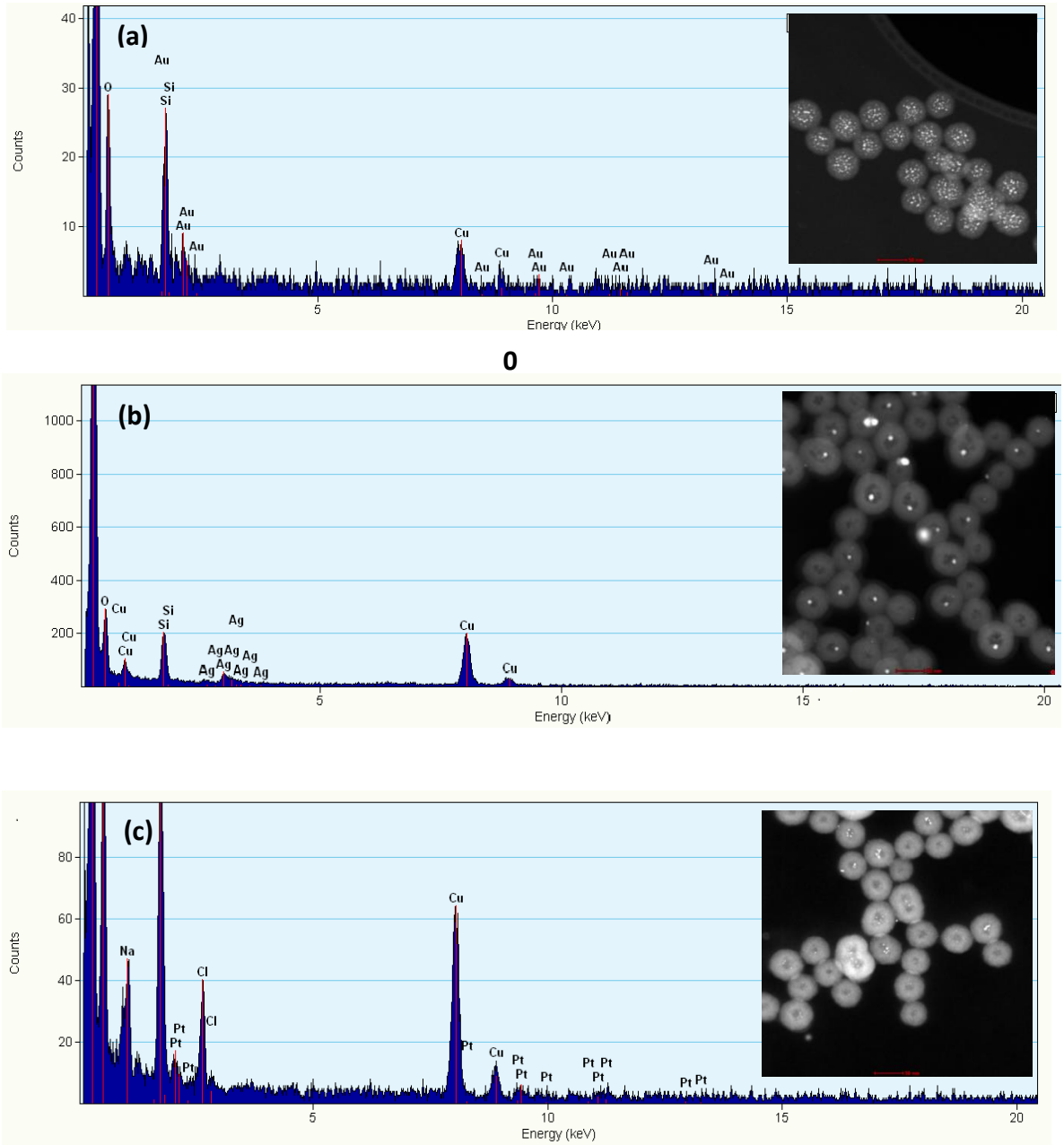

Fig. 23. STEM images and EDX analysis of a) gold, b) silver and c) platinum nanohybrids.

These hybrid nanostructures mantained fluorescence emission showing a maximun peak around 520 nm corresponding with the maximum of FITC-APTES conjugate. However, Fig. 24a shows that this peak is displaced a few nanometers for the different hybrids, due to the possible effect of metal nanoparticles in the emission process. UV-Vis spectra was used as characterization technique of these nanohybrids. As Fig. 24b shows, nanohybrids have a maximum absorption peak around 500 nm corresponding with the maximun absorption peak of FITC-APTES conjugate. Also, in

the case of $Ag@SiO_2$ nanohybrids a characteristic absorption peak around 400 nm was observed corresponding to silver nanoparticles.

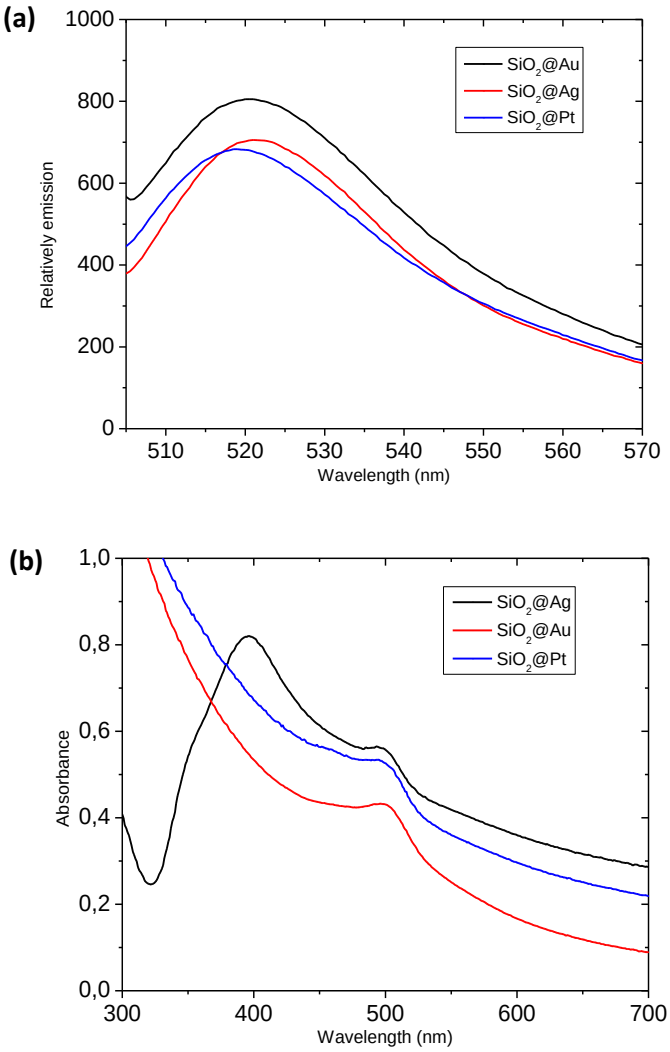

Fig. 24. a) Emission and b) absorption spectra of different metal nanohybrids.

In the second approach, Fe_xO_y silica-based nanohybrids were obtained (Fig. 25). These structures showed magnetic properties because they were attracted by magnet, however they did not show emission properties because during the microwave treatment the fluorophore was destroyed. In that case, different morphologies were obtained and SiO2 matrix was decorated with Fe_xO_y nanoparticles both on the surface and in the inner part of the nanoparticles. This may be related to the ineficient entrance of benzyl alcohol inside the silica nanoparticles before the microwave treatment.

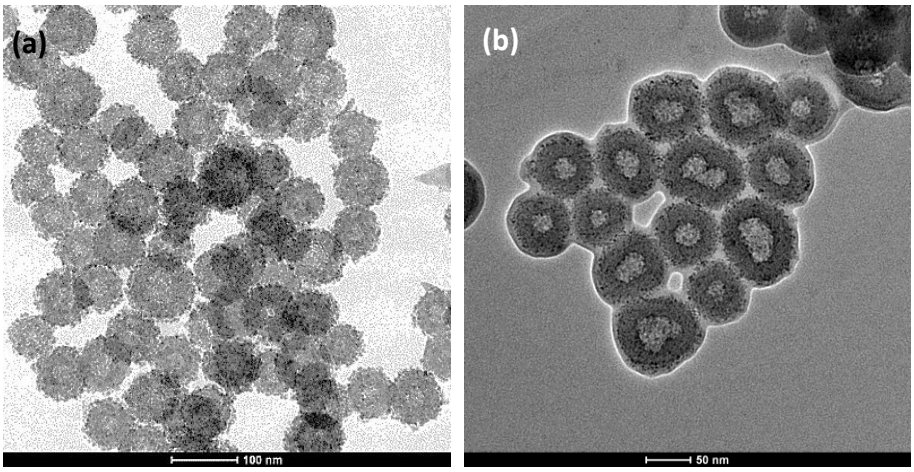

Fig. 25. Two different samples of Fe_xO_y silica-based nanohybrids.

All of synthesized nanohybrids were characterized by XPS in order to check the presence and the atomic percentage of different metal nanoparticles in their structure. By this technique we can check that Fe_xO_y silica nanohybrids were not only formed by iron oxides compounds, if not, the presence of metal iron nanoparticles was detected.

According to TEM images and XPS results (*see annex 2*) iron nanohybrids show metal nanoparticles both on their surface (6.95%) as inside them (9.17%), however in the case of gold, silver and platinum nanohybrids the most part of metal nanoparticles is located inside their nanostructure (0.34%, 0.15% and 0.10% respectively), not on the surface.

4.3 APPLICATIONS

Up to now, diverse applications of silica-based nanohybrids have been reported: $Ag@SiO_2$ nanohybrids can be used taking advantage of their optical properties such as a characteristic surface plasmon resonance. This property allows the use of $Ag@SiO_2$ nanohybrids in different applications such as coating material for solar cells.[22] On the other hand these nanostructures improve the optical signals of other species such as quantum dots photoluminescence,[23] in this way, they can be used in different detection devices, for example, to detect highly reactive oxygen species.[24] $Au@SiO_2$ and $Pt@SiO_2$ has been used as nanoreactors for catalytic reactions. Silica-coated metal catalysts show high resistibility to the sintering of metal at thigh temperatures, because each particles of metal was uniformly covered with silica layers. Also, the selectivity in the catalytics reaction can be improved. In this way, $Pt@SiO_2$ has been used for the competitive oxidation of methane and other higher hydrocarbons with gaseous oxygen[25]

and SiO_2@Au in the reduction of p-nitrophenol to 4-aminophenol.[26,27] Finally, iron oxide nanoparticles can be stabilized by different substrates, such silica, and due to their magnetic behaviour can be used in biological applications such as a contrast agent in magnetic resonance image (MRI), drug delivery, *in vitro* separation or hyperthermia.[28]

In addition to primary objetive in this final master project, the potential use of the synthesized nanohybrids was explored in order to provide the basis of a further development of those silica-bsed nanostructures.

Au@SiO_2 nanohybrids suspension showed characteristic red colour due to gold nanoparticles capable to absorbe ligth at 540 nm. A sample (0.83 mg/mL) was submitted at laser radiation at this wavelength during 15 min and we could observe a sligth increase of the temperature. This increase was very weak, possibly due to the small concentration of gold nanoparticles (*see annex 3*). Moreover, set of experiments were done to check the catalytic performance of synthesized Au@SiO_2 nanohybrids in the reduction of p-nitrophenol to 4-aminophenol which was followed by UV-Vis. However prelliminary result were not conclusive. A broader work would be necessary to determine their potential as catalyst. On the other hand, further optimization work could be done related the amount of gold loaded in these nanorattles in order to use these nanostrucutres in hyperthermia treatment. This together with their fluorescent characteristic make them an interesting multifunctional nanostructures.

In the case of Ag@SiO_2 and Pt@SiO_2, future work is based on improve the metal loading process in order to obtain nanohybrids with higher atomic percentage of metal nanoparticles inside the nanohybrids. Moreover, the possibility to obtain a controlled silver ions release by the application of a laser radiation will be addressed to take advantage of their bactericide properties in different media. Also, the surface enhanced Raman spectroscopy (SERS) due to the optical properties of Ag@SiO_2 and Au@SiO_2 should be tested. Optimization of the synthesis method of Fe_xO_y silica-based nanohybrids will be carried out and their magnetic behaviour will be studied by Superconducting Quantum Interference Devices (SQUID).

In all cases, their toxicity must be analyzed in order to check if these nanostrcutres could be used in biomedical applications.

5. CONCLUSIONS

In this work, we present one-step synthesis of monodisperse silica-coated nanohybrids by means of in situ growth of nanoparticles cores during the hollow silica nanoparticles formation by w/o microemulsion.

A mechanism for the formation of fluorescent hollow silica nanoparticles was proposed. And it has allowed us to tailor the synthesis of SiO_2-based hollow nanoparticles by controlling the synthesis and aging conditions.

Last but not least, we were able to introduce different useful loads as metal nanoparticles taking advantage of the knowledge acquired of the hollowing process of SiO_2 nanoparticles. As a result, functionalized silica-based nanostructures useful for different applications were obtained by a simple method.

6. REFERENCES

1. G. Cao, *Nanostructures and Nanomaterials. Synthesis, Properties and Applications.* Imperial College Press, 2004
2. http://www.nanotecnologia.cl
3. www.scopus.com
4. D. Carmona.PhD Thesis, Universidad de Zaragoza, 2013.
5. C.J. Brinker et al. *Sol-gel scince.* Academic Press, 1990.
6. K. Natte.. PhD Thesis. University of Berlin, 2013.
7. W. Stöber et al. Journal of Colloid and Interface Science, 26, 62-69, 1968.
8. D. Knopp et al. Analytica Chimica Acta, 647, 14-30, 2009.
9. R. P. Bagwe et al. Langmuir, 22, 9, 4357–4362, 2006.
10. K. Wegner et al. Chemical Engineering Science, 5,4581-4589, 2003.
11. W. Teoh et al. Nanoscale, 2, 1324-1347, 2010.
12. M. Llinas et al.Afinidad LXXI, 565, 20-31, 2014.
13. Y. Wang et al.Nanomedicine: Nanotechnology, Article in Press, 2014
14. S. Santra et al. Anal. Chem. 73, 4988-4993, 2001.
15. S. Santa, B. et al. Journal of Luminescence 117, 75-82, 2006.
16. Z. Li et al. Journal of Controlled Release 98, 245-254, 2004.
17. J. Lee et al. Nanotoday 9, 631-667, 2014.
18. S. Santra et al.Chem. Commun. 2810-2811, 2004.
19. Y. Jin et al. Coordination Chemisty Reviews 253, 2998-3014, 2009.
20. I. Bilecka et al. *One-minute synthesis of crystalline binary and ternary metal oxide nanoparticles.*Chem. Commun., 886-888, 2008.
21. R. Sjöback et al.Spectrochimica Acta Part A, 51, L7-L21, 1995.
22. T. Gao et al. Nanopart Res, 15:1370, 1-9, 2013.
23. Y. Chang et al. 2013.
24. H. Wang et al. American Chemical Society, 86, 3013-3019,2014.
25. K. Hori et al. Science and Technology of Advanced Materials 7, 678-684, 2006.
26. J. Lee et al. Adv. Mater. 20, 1523-1528, 2008.
27. V. Evangelista et al. Applied Catalysis B: Environmental, 166-167, 518-528, 2015.
28. S. Laurent et al. Chemical Reviews, 108, 2064-2110, 2008.

7.ATTACHMENTS

7.1. ^{1}H-NMR SPECTRA

^{1}H-NMR spectra corresponding to different species in deuterated methanol has been showed below:

APTES

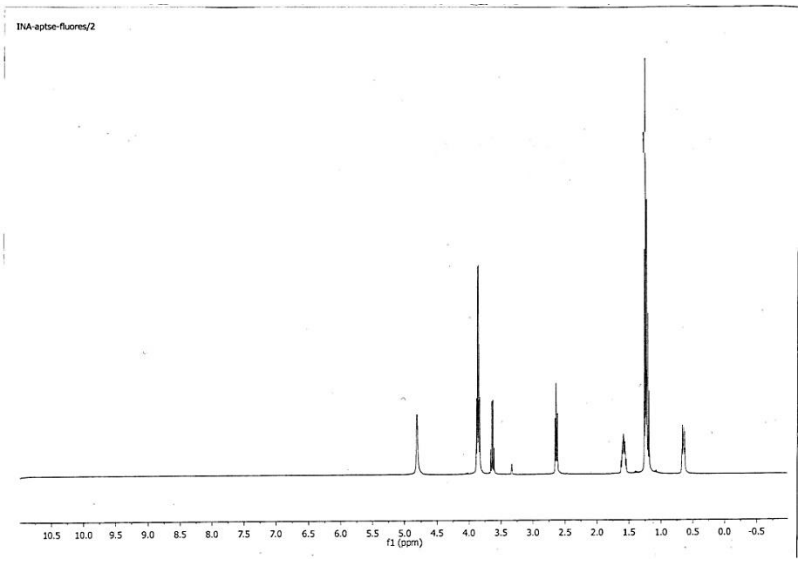

FITC

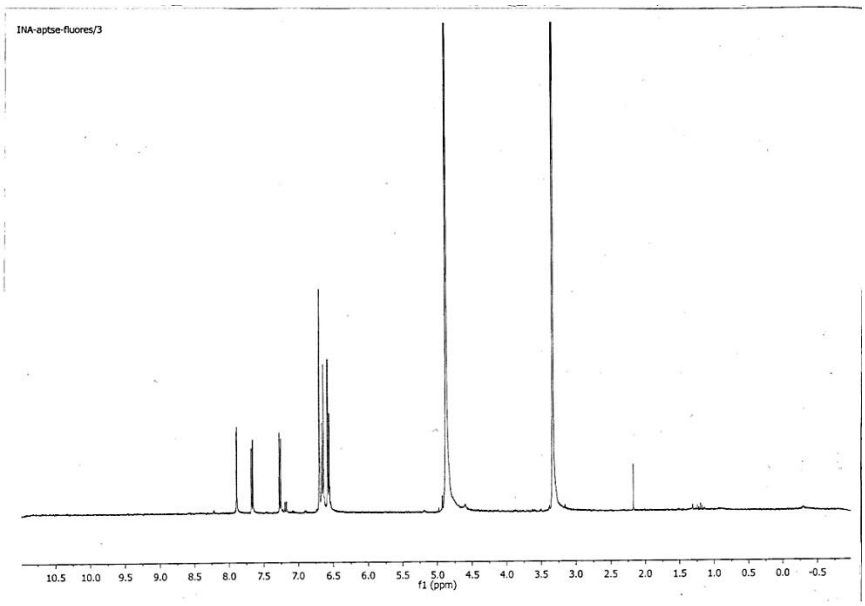

APTES-FITC CONJUGATE

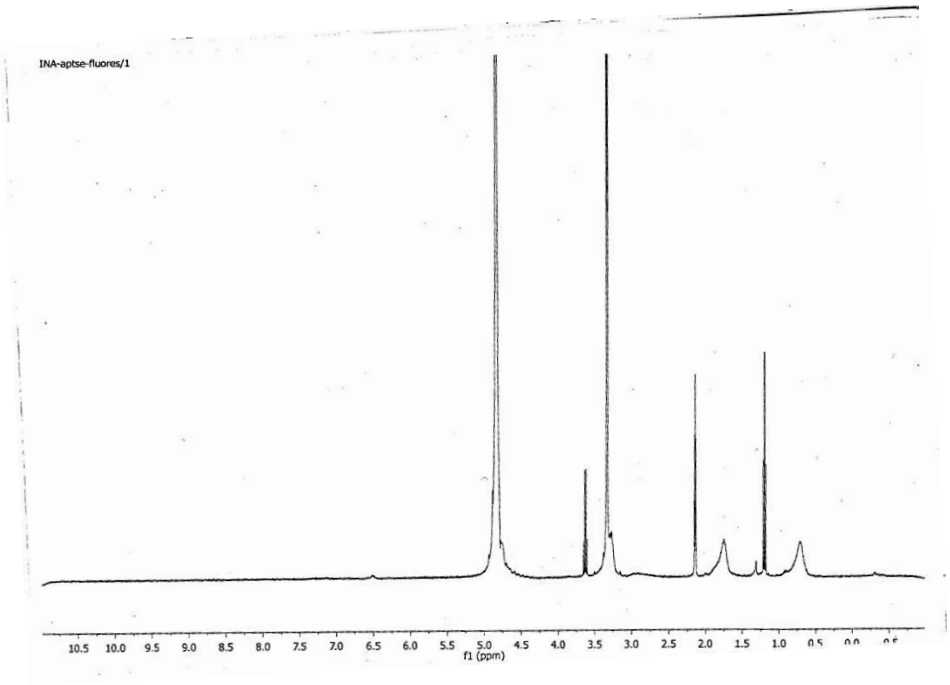

SUPERNATANT

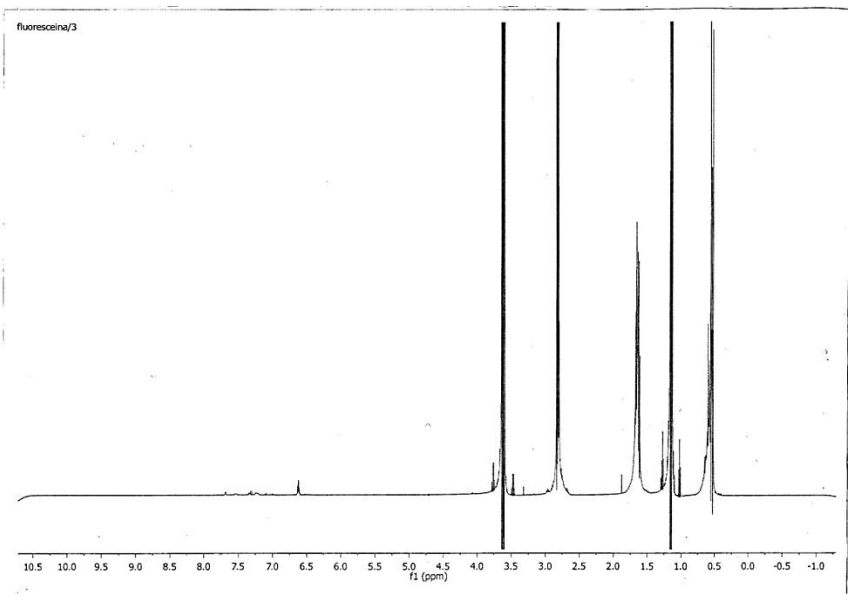

7.2. XPS RESULTS

The following table shows the results obtained in XPS experiment for metal-silica nanohybrids.

	C 1s	O 1s	Si2p	Metal
Pt/SiO2	74.98	21.60	3.41	0
	58.21	26.38	15.32	0.09
	62.92	22.06	14.91	0.11
	67.71	19.25	12.93	0.10
	68.42	18.81	12.66	0.10
	67.59	19.29	13.01	0.10
Ag/SiO2	76.74	20.54	2.64	0.07
	76.43	14.72	8.69	0.16
	80.47	12.01	7.38	0.13
	79.89	12.83	7.16	0.12
	82.72	10.57	6.58	0.12
	81.73	11.20	6.91	0.15
Fe/SiO2	73.44	22.97	2.58	1.00
	85.68	5.60	1.76	6.95
	88.37	4.19	1.01	6.42
	87.14	4.35	0.76	7.74
	89.61	2.98	0.24	7.17
	89.71	3.20	0.19	6.89
	89.22	3.14	0.37	7.27
	88.65	2.49	0.35	8.505
	88.84	2.38	0.08	8.69
	88.13	2.69	0	9.17
Au/SiO2	75.43	21.21	3.35	0
	52.20	28.99	18.45	0.36
	54.66	27.31	17.68	0.34
	60.49	24.21	15.03	0.27
	61.74	22.70	15.28	0.27
	62.11	22.35	15.24	0.30
	62.42	22.84	15.43	0.30
	60.58	22.97	16.14	0.30
	62.07	21.57	16.03	0.33
	60.00	24.14	15.52	0.34

7.3 LASER EXPERIMENT

The following graph show the increase of temperature when a sample of $Au@SiO_2$ was irradiated by a laser at 540 nm. The graph shows a weak increase in the temperature due to absorbed radiation by gold nanoparticles.